# Steady-State Response of a Multidegree System With an Impact Damper

Sami Masri

# Steady-State Response of a Multidegree System With an Impact Damper

**S. F. MASRI**
Associate Professor,
Department of Civil Engineering,
University of Southern California,
Los Angeles, Calif.

*An exact solution is presented for the steady-state motion of a sinusoidally excited n-degree-of-freedom system that is provided with an impact damper. Both the excitation and the damper may be independently applied to any point in the system. Experimental studies with an analog computer and with a mechanical model corroborate the theoretical results. Results of the analysis are applied to the lumped parameter representation of a modern 10 story building, and the effects of various system parameters, including mode shape, excitation frequency, damper location, and force location are determined. It is found that the impact damper is an efficient device for reducing the vibrations of multidegree-of-freedom systems, particularly in structures such as tall buildings.*

RECENT studies [1, 2][1] have shown that chain-type impact dampers offer a simple and reliable method for attenuating wind-induced vibrations of tall flexible structures such as launch vehicles, antennas, smoke stacks, etc. However, although impact dampers have been investigated both analytically and experimentally, no analytical results are available in the literature regarding the response of multidegree-of-freedom systems utilizing impact dampers. It will be shown in this paper that the use of impact vibration dampers is feasible to suppress earthquake-induced or wind-induced oscillations of tall buildings.

This paper presents the exact solution for the steady-state motion of a series-type multidegree-of-freedom system equipped with an impact damper and subjected to a sinusoidal force input. The lumped parameter model of the $n$-degree-of-freedom system being considered is shown in Fig. 1. The sinusoidal forcing function is applied to the $k$th mass and the impact damper is attached to the $j$th mass. It is assumed that, during a period of the forcing function, two symmetric impacts occur at equal time intervals and at opposite ends of the damper container. This assumed motion is consistent with that which has been found to predominate in the experimental studies of impact dampers as observed by most investigators in this field.

## Steady-State Solution

The equation of motion of the system in the absence of the damper is

$$[m]\ddot{\mathbf{x}} + [c]\dot{\mathbf{x}} + [k]\mathbf{x} = \mathbf{F}(t) \tag{1}$$

where $[m]$, $[c]$, $[k]$ are the mass, damping, and stiffness matrices, respectively, and $\mathbf{F}(t) = \text{col}\{0, 0, \ldots, 0, F_k(t), 0, \ldots, 0\}$.

Assume that the damping mechanism is the proportional-type satisfying the condition

$$[c] = \alpha[m] + \beta[k] \tag{2}$$

where $\alpha$ and $\beta$ are constants.

Consider the steady-state motion of the system shown in Fig. 1 with the origin of the time axis shifted to coincide with the time of occurrence of an impact at $t = t_0$. The result of this shift is to modify the excitation force, giving in the new time scale

$$F_k(t) = F_0 \sin(\Omega t + \alpha_0) \tag{3}$$

where $\alpha_0 \equiv \Omega t_0$ is a phase angle to be determined from the steady-state motion.

Using the normal mode approach, equation (1) can be transformed into the form

$$[\diagdown M \diagdown]\ddot{\mathbf{q}} + [\diagdown C \diagdown]\dot{\mathbf{q}} + [\diagdown K \diagdown]\mathbf{q} = \mathbf{Q}_{ex}(t) \tag{4}$$

where the $n$-components of $\mathbf{q}$ are the normal coordinates, $[\diagdown M \diagdown]$, $[\diagdown C \diagdown]$, and $[\diagdown K \diagdown]$ are diagonal matrices corresponding to the

---

[1] Numbers in brackets designate References at end of paper.

Contributed by the Applied Mechanics Division and presented at the Applied Mechanics Summer Conference, University of California, La Jolla, Calif., June 26–28, 1972, of THE AMERICAN SOCIETY OF MECHANICAL ENGINEERS.

Discussion on this paper should be addressed to the Editorial Department, ASME, United Engineering Center, 345 East 47th Street, New York, N. Y. 10017, and will be accepted until April 20, 1973. Discussion received after this date will be returned. Manuscript received by ASME Applied Mechanics Division, September, 1971; final revision, January, 1972. Paper No. 72-APM-39.

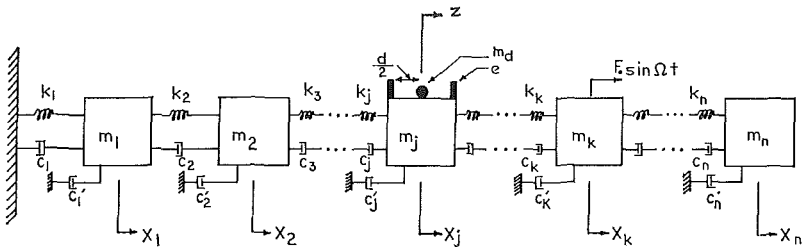


**Fig. 1 Model of system**

generalized mass, damping, stiffness matrices, respectively, and where $\mathbf{Q}_{ex}(t) = [\varphi]^T \mathbf{F}(t)$, and $[\varphi]$ is the modal matrix.
The $i$th equation of system (4) is

$$M_i \ddot{q}_i + C_i \dot{q}_i + K_i q_i = Q_{ex,i} \equiv \varphi_{ki} F_0 \sin (\Omega t + \alpha_0) \quad (5)$$

and its solution is

$$q_i(t) = \exp\left(-\frac{\zeta_i}{r_i}\Omega t\right)\left\{\frac{1}{\eta_i}\left(\zeta_i \sin\frac{\eta_i}{r_i}\Omega t + \eta_i \cos\frac{\eta_i}{r_i}\Omega t\right) q_{0i} + \frac{1}{\omega_i \eta_i}\left(\sin\frac{\eta_i}{r_i}\Omega t\right)\dot{q}_{ai} - \frac{A_i}{\eta_i}\left(\zeta_i \sin\frac{\eta_i}{r_i}\Omega t + \eta_i \cos\frac{\eta_i}{r_i}\Omega t\right)\sin\tau_i - \frac{A_i}{\eta_i} r_i \left(\sin\frac{\eta_i}{r_i}\Omega t\right)\cos\tau_i\right\} + A_i \sin(\Omega t + \tau_i)$$

$$i = 1, 2, \ldots, n \quad (6)$$

where

$$\omega_i \equiv \sqrt{\frac{K_i}{M_i}} \qquad \zeta_i \equiv \frac{C_i}{\sqrt{2K_i M_i}}$$

$$\eta_i \equiv \sqrt{1 - \zeta_i^2} \qquad r_i \equiv \frac{\Omega}{\omega_i}$$

$$f_i \equiv \varphi_{ki} F_0 \qquad A_i \equiv \frac{f_i/K_i}{\sqrt{(1 - r_i^2)^2 + (2\zeta_i r_i)^2}}$$

$$\Psi_i \equiv \tan^{-1}\frac{2\zeta_i r_i}{1 - r_i^2} \qquad \tau_i \equiv \alpha_0 - \Psi_i$$

$$q_{0i} \equiv q_i(0) \qquad \dot{q}_{ai} \equiv \dot{q}_i(0_+)$$

and the + subscript indicates conditions immediately after the specified time. Letting the initial displacement and velocity at $t = 0_+$ be

$$\mathbf{x}(0) \equiv \mathbf{x}_0 = [\varphi]\mathbf{q}_0, \qquad \dot{\mathbf{x}}(0_+) \equiv \dot{\mathbf{x}}_a = [\varphi]\dot{\mathbf{q}}_a \quad (7)$$

then

$$\mathbf{x}(t) = [B_{21}(t)]\dot{\mathbf{x}}_a + [B_{22}(t)]\mathbf{x}_0 + [B_{23}(t)]\mathbf{S}_1 + [B_{24}(t)]\mathbf{S}_2 + [\varphi]\mathbf{S}_3(t) \quad (8)$$

$$\dot{\mathbf{x}}(t) = [B_{31}(t)]\dot{\mathbf{x}}_a + [B_{32}(t)]\mathbf{x}_0 + [B_{33}(t)]\mathbf{S}_1 + [B_{34}(t)]\mathbf{S}_2 + [\varphi]\mathbf{S}_4(t) \quad (9)$$

where the undefined matrices and vectors are functions of the system parameters.

Letting $y(t)$ be the relative displacement of the damper mass $m_d$ with respect to $m_j$, then

$$y(t) = z(t) - x_j(t). \quad (10)$$

Since the time origin coincides with the time of occurrence of an impact,

$$y(0) \equiv y_0 = z(0) - x_j(0) = \pm\frac{d}{2} \quad (11)$$

During an impact (idealized to be a discontinuous process), the conditions of the system remain unchanged except for the velocities of $m_d$ and $m_j$, whose instantaneous changes are calculated using the momentum equation and the coefficient of restitution. Noting that in steady-state motion

$$\dot{z}(0)_+ = -\frac{2\Omega}{\pi}(x_{0j} + y_0) \quad (12)$$

then the velocity vectors before and after an impact are related by

$$\dot{\mathbf{x}}_b = [\lfloor B_6 \rfloor]\dot{\mathbf{x}}_a \quad (13)$$

## Nomenclature

- $m_i$ = $i$th mass in multidegree-of-freedom system
- $k_i$ = $i$th spring constant in multidegree-of-freedom system
- $\alpha, \beta$ = constants used to specify proportional-type damping
- $x_i(t)$ = absolute displacement of $i$th mass
- $\dot{x}_i(t)$ = absolute velocity of $i$th mass
- $z(t)$ = absolute displacement of damper $m_d$
- $y(t)$ = relative displacement of damper with respect to mass $m_j$
- $m_d$ = damper mass
- $F_0$ = amplitude of sinusoidol exciting force $F_0 \sin \Omega t$
- $\Omega$ = frequency of sinusoidol excitation $F_0 \sin \Omega t$
- $\alpha_0$ = phase angle, initially unknown
- $\omega_i$ = $i$th natural frequency of multidegree-of-freedom system
- $\zeta_i$ = ratio of critical damping corresponding to $i$th mode
- $\mu_T$ = mass ratio of damper to total mass of structure, $m_d / \sum_{i=1}^{n} m_i$
- $\mu$ = mass ratio of damper to mass $m_j$ to which it is attached, $m_d/m_j$
- $e$ = coefficient of restitution
- $d$ = clearance in which damper is free to oscillate
- $j$ = mass number to which damper is attached
- $k$ = mass number to which force is applied
- $n$ = total number of masses in $n$-degree-of-freedom system
- $x_{sti}$ = static deflection of $i$th mass in an $n$-degree-of-freedom system when force is applied to mass $m_k$
- $x_{pi}$ = peak displacement amplitude of mass $m_i$ in the absence of damper
- $x_{maxi}$ = maximum displacement amplitude of mass $m_i$ with damper operating

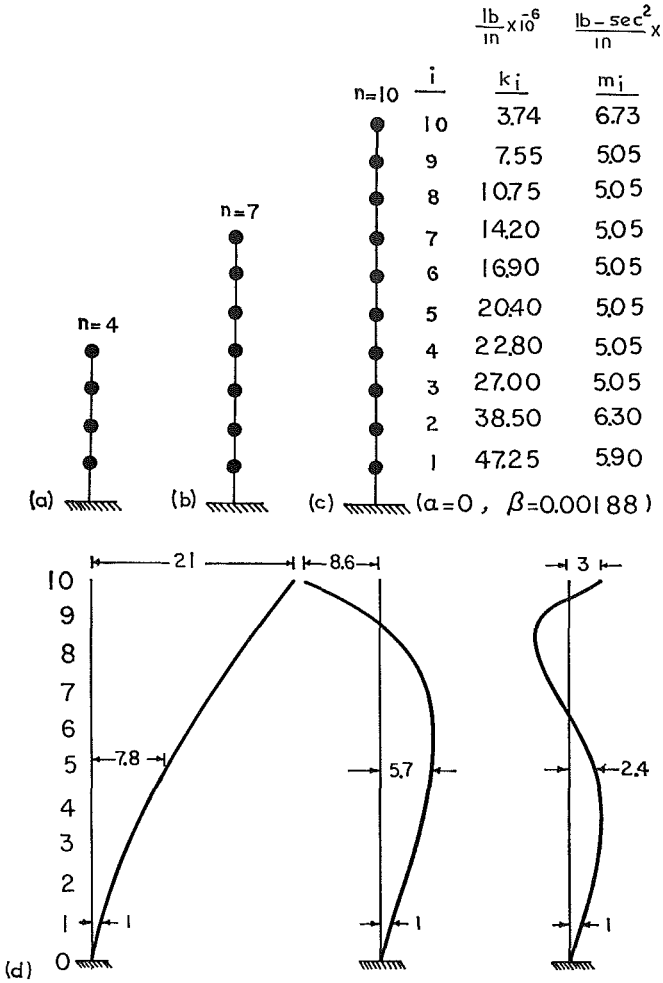


**Fig. 2 Example structure: (a) four-degree-of-freedom system; (b) seven-degree-of-freedom system; (c) 10-degree-of-freedom system; (d) first three modes of 10-degree-of-freedom system**

where $[\searrow B_6 \searrow]$ is a constant diagonal matrix whose elements are equal to unity, except for the $j$th element which is equal to $(1 - e - 2\mu)/(1 - e - 2\mu e)$.

In steady-state motion with two symmetric impacts/cycle of excitation on opposite ends of damper container,

$$\mathbf{x}(t)\big|_{\Omega t=\pi} = -\mathbf{x}(0) = -\mathbf{x}_0 \tag{14}$$

$$\dot{\mathbf{x}}(t)\big|_{\Omega t=\pi_-} = -\dot{\mathbf{x}}(0)_- = -\dot{\mathbf{x}}_b = -[\searrow B_6 \searrow]\dot{\mathbf{x}}_a \tag{15}$$

Using (14) and (15) in conjunction with (8) and (9)

$$\mathbf{x}_0 = \mathbf{S}_7 \sin \alpha_0 + \mathbf{S}_8 \cos \alpha_0 \tag{16}$$

$$\dot{\mathbf{x}}_a = \mathbf{S}_9 \sin \alpha_0 + \mathbf{S}_{10} \cos \alpha_0 \tag{17}$$

Equations (16) and (17), together with (13), result in

$$\alpha_0^{\pm} = \tan^{-1}[(h_1h_3 \pm h_2h_4)/(h_2h_3 \mp h_1h_4)] \tag{18}$$

where the $h$'s are functions of $\mathbf{S}_7 - \mathbf{S}_{10}$. With $\alpha_0$ determined from (18), the rest of the unknowns can be found by back substitution.

## Applications

Consider the 10-degree-of-freedom lumped parameter system shown in Fig. 2($c$) whose natural frequencies, mode shapes, and damping characteristics approximate those obtained experimentally from full-scale dynamic tests of a modern 10-story building [3].

To investigate the effects of various system parameters, the models shown in Figs. 2($a$) and ($b$) were also studied. The hypothetical systems in Figs. 2($a$) and ($b$) consist of the first 4 and first 7 stories, respectively, of the system in Fig. 2($c$). Fig. 2($d$) shows the first three mode shapes and the corresponding frequencies for the lumped parameter representation of the 10-story building in Fig. 2($c$).

Fig. 3 shows a typical solution curve for the 7-story building in Fig. 2($b$). The left-hand-side (LHS) ordinate in Fig. 3 is the ratio of the maximum displacement of the $i$th floor, $x_{\max i}$, for the structure using the damper divided by the peak displacement, $x_{pi}$, of the same floor with no damper being used. This ratio is, therefore, a measure of the effectiveness of the damper (without a damper the solution curve is a straight line at $x_{\max i}/x_{pi} = 1$). The abscissa in Fig. 3 is the clearance ratio $d/x_{st_n}$, where $x_{st_n}$ is the static deflection of the top floor with the excitation force and the damper both applied at the top.

For a given set of parameters there are two possible solutions to equation (18) labeled $\alpha_0^+$ and $\alpha_0^-$, which correspond to two distinct steady-state solutions. Experiments with an electronic analog computer were conducted to check the theoretical results and to determine which branch of the solution, if any, was asymptotically stable. As indicated by the experimental results shown in Fig. 3, the solution curve associated with $\alpha_0^+$ (which, in general, leads to lower response amplitude than solution curve $\alpha_0^-$) was found to be stable throughout most of its range.

The validity of the analytical results were further compared to, and were found to be in excellent agreement with, published

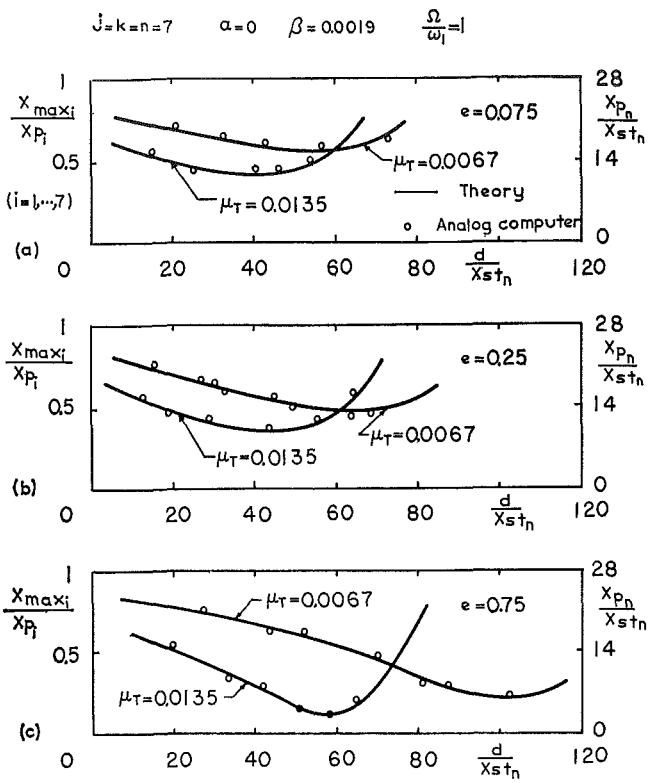


**Fig. 3 Comparison of analytical and experimental results; $j = k = n = 7$; $\Omega/\omega_1 = 1$—(a) $e = 0.075$; (b) $e = 0.25$; and (c) $e = 0.75$**

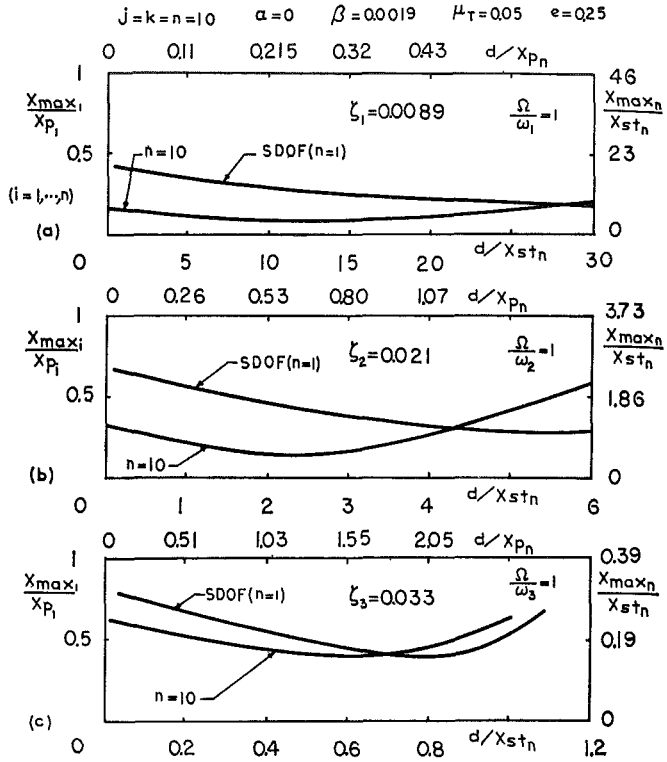


**Fig. 4 Effects of mode shape: $j = k = n = 10$, $\mu_T = 0.05$, $e = 0.25$—(a) $\Omega/\omega_1 = 1$; (b) $\Omega/\omega_2 = 1$; and (c) $\Omega/\omega_3 = 1$**

analytical and experimental results pertaining to single-degree-of-freedom systems provided with impact dampers [4].

**Effects of System Parameters.** A detailed investigation of the independent parameters on the response of the system was undertaken, and the results can be summarized as follows:

1 **Mass Ratio $\mu_T$.** The system under discussion is effective even with mass ratios on the order of 1 percent. Note from Fig. 3 that even with a mass ratio $\mu_T \approx 0.005$ the response amplitude can be reduced by as much as 80 percent.

For "tall" structures operating in the vicinity of their first mode, similar to the one under discussion, the optimum clearance ratio (in regard to vibration attenuation) satisfies the condition $\mu_T d/x_{st_n} \approx 0.6$ and results in a reduced amplitude which satisfies the relationship $\mu_T x_{max_i}/x_{p_i} \approx 0.001$, $(i = 1, 2, \ldots, n)$ for relatively high values of $e$.

2 **Natural Mode Shapes.** The response of the 10-story building under discussion vibrating in each of its first three modes is given in Fig. 4. It can be seen that, with a given damper mass, the maximum percentage reduction in the response of the structure is achieved in the first mode. The maximum reduction decreases with mode number from 90 percent in the first, to 85 percent in the second, and 60 percent in the third. One of the reasons for this reduction in the efficiency of the damper is that $\zeta_i$, the ratio of critical damping in the $i$th mode, increases with mode number from $\zeta_1 \approx 0.01$ to $\zeta_2 \approx 0.02$ and $\zeta_3 \approx 0.03$. Figs. 4($a$), ($b$), and ($c$) also show the corresponding response of an equivalent single-degree-of-freedom (SDOF) system whose ratio of critical damping is the same as the 10-story building in a given mode. It is clear from Fig. 4 that factors in addition to damping are involved in modifying the performance of the damper. Since the "moment arm" of the damper with respect to the base of the building is not affected by the mode shape, it appears that the main factor that influences the efficiency of the damper is the magnitude of the displacement of $m_j$ to which the damper is attached.

3 **Damper Location $j$.** Fig. 5 illustrates some of the possible

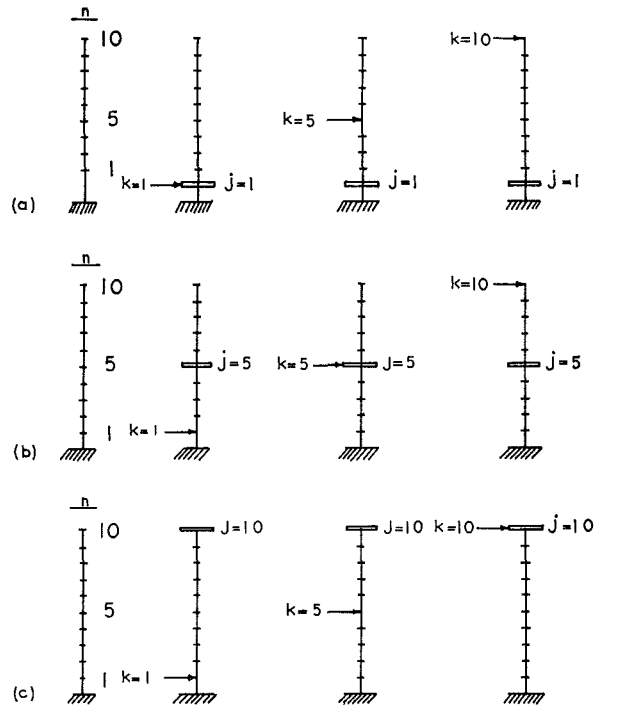


**Fig. 5 Different combinations of force and damper location for 10-story building; (a) $j = 1$; (b) $j = 5$; and (c) $j = 10$**

damper locations in the 10-story ($n = 10$) building that is vibrating in its first mode.

With the force imposed on mass $m_5$ (i.e., $k = 5$), then, for the parameters in Fig. 6, the maximum reduction in amplitude will be ≈2 percent if the damper is attached to $m_1$, Fig. 6($a$), about 50 percent if the damper is at $m_5$, Fig. 6($b$), and more than 90

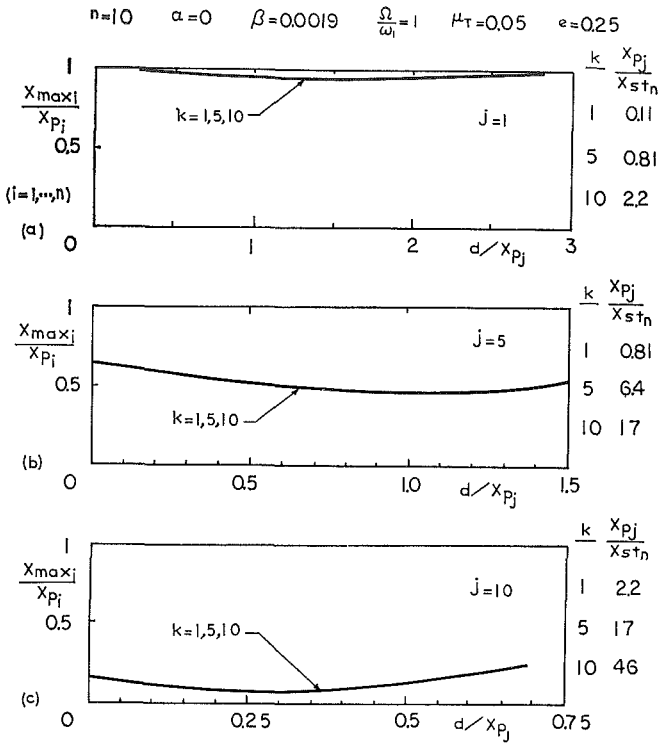


Fig. 6 Effects of force and damper location: $n = 10$, $\Omega/\omega_1 = 1$, $\mu_T = 0.05$, $e = 0.25$; (a) $j = 1$; (b) $j = 5$; and (c) $j = 10$

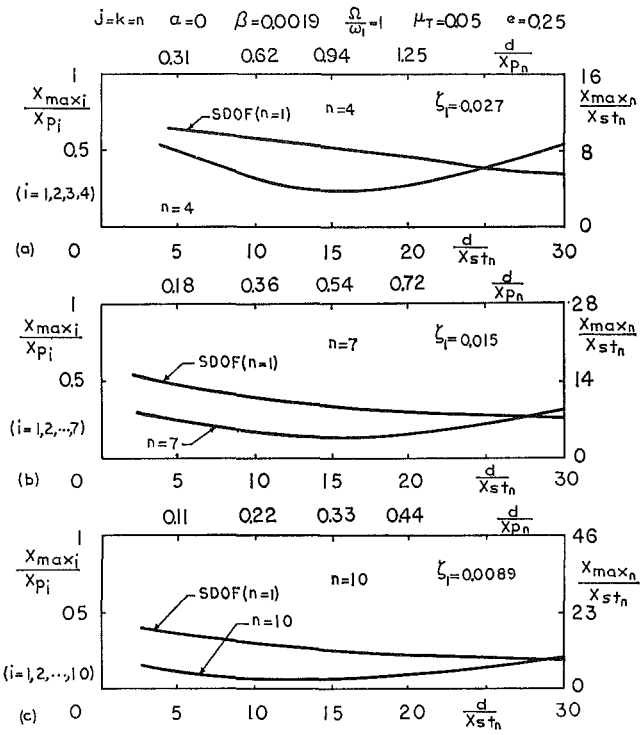


Fig. 7 "Telescoping" effect: $\Omega/\omega_1 = 1$, $\mu_T = 0.05$, $e = 0.25$, $j = k = n$; (a) $n = 4$; (b) $n = 7$; and (c) $n = 10$

percent if the damper is placed at the top floor, Fig. 6(*c*). This progressive increase in efficiency with the damper "elevation" above the ground floor is to be expected since the moment arm increases with increasing $j$ to a maximum at the top floor (i.e., $j = n$).

For modes other than the first, increase in moment arm must be modified to account for the relative locations of the damper and the nodal points.

**4 Force Location *k*.** Although the application of an exciting force of a given amplitude at different points along the structure will affect the magnitude of the response of the structure, it was found that the response curves for an impact damped structure are virtually independent of the point of application of the exciting force, provided that the results are expressed in terms of $d/x_{pj}$ and $x_{\max i}/x_{pi}$.

**5 Telescopic Effect.** Fig. 7 shows the relation between the amplification ratio $x_{\max i}/x_{st_i}$, $(i = 1, \ldots, n)$ and the clearance ratio $d/x_{st_n}$ for the three buildings shown in Fig. 2, where each one is vibrating in its first mode and with both force and damper acting on the top floor so that $j = k = n$.

It is clear that if the damper mass ratio $\mu_T$ is kept constant, the effectiveness of the damper is proportional to the height of the building. This is due to the fact that as the height of the building is increased, the moment arm of the impact damper is simultaneously increased to amplify the dampening effects. The deviation of the results from the corresponding ones for an equivalent SDOF system increases as the number of stories increase.

**6 Damping in the Primary System ($\alpha, \beta$).** An increase in the viscous damping of the primary system is detrimental to the efficiency of the impact damper.

**7 Excitation Frequency Ω.** If the structure is excited at a fixed frequency, the design parameter can be optimized according to the aforementioned criteria. However, if the response is to be controlled effectively over a relatively wide frequency band, an increase in $\mu_T$ and damping or a decrease in $e$ will improve the performance of the damper.

**8 Base Excitation.** The present theory can also analyze cases where the excitation is supplied through support displacement rather than force excitation. The base-excited two-degree-of-freedom system in Fig. 8(*a*) is equivalent to the force-excited three-degree-of-freedom system in Fig. 8(*b*) where $m_1$ replaces the support and the excitation amplitude is adjusted so that $S_0/(F_0/k_1) = 1$.

The theoretical predictions and the corresponding experimental measurements obtained by using an actual mechanical model are shown in Fig. 8(*c*). As mentioned earlier, of the two possible steady-state solutions, the one associated with $\alpha_0^+$ is the stable one. This is true in spite of the fact that, for the case in the frequency range $\Omega/\omega_1 \lesssim 0.95$, the solution $\alpha_0^+$ leads to larger amplitudes than $\alpha_0^-$. Note also the existence of a peak in the response curve at $\Omega/\omega_1 \approx 1/(1 + \mu_T)$.

**Practical Design Considerations.** Some of the design problems inherent in the application of practical impact dampers are (*a*) large accelerations developed during impact; (*b*) the accompanying noise; (*c*) design of the concentrated impacting mass (in massive structures, such as buildings, even a damper mass ratio of $\approx$1 percent is still a large weight to have suspended in the structure). Analytical and experimental studies have shown that the foregoing problems can be alleviated to some extent by the use of multiple-unit impact dampers operating in parallel, instead of one single "particle."

## Summary and Conclusions

An exact theory is presented for determining the steady-state motion of a damped multidegree-of-freedom lumped parameter system that is provided with an impact damper attached to some arbitrary point in the structure and is subsequently excited by a sinusoidal force, also applied to an arbitrary point.

The results were applied to several multidegree-of-freedom systems, including a model of a modern 10-story building. A detailed investigation of the effects of various parameters of the system on the response was conducted. It was found that regardless of where the excitation is applied (including the base) the efficiency of the damper increases as its moment arm in-

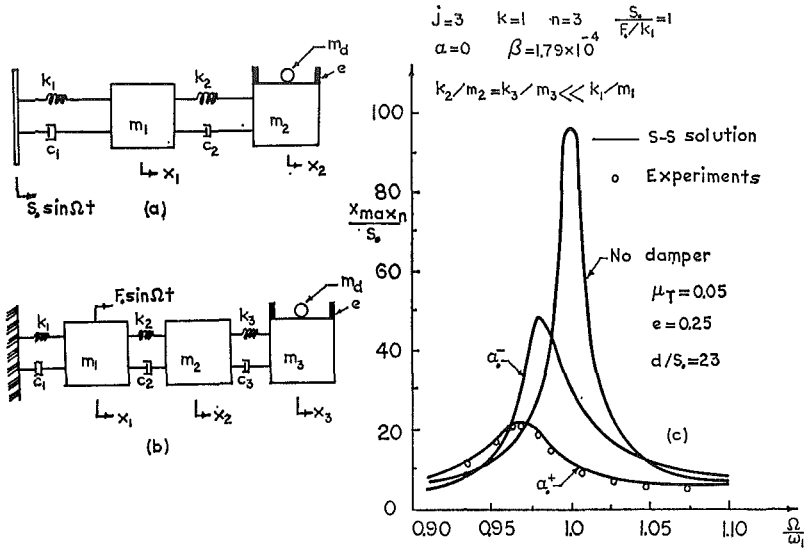


**Fig. 8 Base excitation: (a) base-excited two-degree-of-freedom model; (b) equivalent force excited model; and (c) frequency response of a base-excited two-degree-of-freedom system**

creases. Due to the "telescoping effect," it is feasible to use impact dampers, with mass ratios on the order of 1 percent of the mass of a lightly damped structure, to considerably attenuate the response of the structure over a relatively broad suppression band around any frequency of interest.

Predictions of the theory were corroborated by experimental studies with an electronic analog computer and with a mechanical model.

## Acknowledgment

This work was supported by the National Science Foundation Grant No. GK-11553. The assistance of Dr. D. S. Margolias in the preparation of this manuscript is appreciated.

## References

1 Reed, W. H., III, and Duncan, R. L., "Dampers to Suppress Wind-Induced Oscillations of Tall Flexible Structures," *Developments in Mechanics*, Vol. 4, Cermak, J. E., and Goodman, J. R., eds., Johnson Publishing Co., 1968, pp. 881–897.

2 Reed, W. H., III, "Hanging-Chain Impact Dampers: A Simple Method for Damping Tall Flexible Structures," *Wind Effects on Buildings and Structures*, Vol. II, University of Toronto Press, 1968, pp. 283–321.

3 Kuroiwa, J. H., *Vibration Test of a Multistory Building*, Earthquake Engineering Research Laboratory, California Institute of Technology, Pasadena, Calif., 1967.

4 Masri, S. F., and Caughey, T. K., "On the Stability of the Impact Damper," JOURNAL OF APPLIED MECHANICS, Vol. 33, TRANS. ASME, Vol. 88, Series E, 1966, pp. 586–592.